



Variations in capillary water absorption and porosity of some limestones during weathering due to salt and air pollutants

Sevgi Çetintaş¹ · Metin Bağcı² · Ahmet Yıldız²

Received: 5 July 2022 / Accepted: 25 June 2023 / Published online: 8 July 2023
© The Author(s), under exclusive licence to Springer-Verlag GmbH Germany, part of Springer Nature 2023

Abstract

As a building material, limestone is affected salt and acid solutions resulting from intense weather conditions over time. In the present study, variations in capillary water absorption, porosity, physical changes, and internal rock decomposition mechanisms caused by salt crystallization and air pollutants (SO_x and NO_x) in sedimentary limestone from the Antalya region were explored. The mineralogical–petrographical and geochemical properties of the limestones were determined using polarizing light microscopy, scanning electron microscopy (SEM), and X-ray fluorescence methods. The variations in the capillary water absorption coefficient, weight, and pore distribution and size were also determined by mercury porosimetry (MIP). An increase in weight was observed in the salt and SA (150 ± 10 mL deionized water and 500 ± 10 mL H_2SO_3 acid) weathering tests, but a reduction in weight was found under the action of NA (150 ± 10 mL deionized water and 500 ± 10 mL HNO_3 acid). The reaction of SA with the limestones influenced the presence of calcium sulphite hemihydrate and gypsum on the rock surface, which affected weight gain. A decrease was observed in the weights of the limestones under the action of NA, and the porous structure seen in the microscale examination from SEM analysis supported a loss of material. The values for capillary water absorption increased in the limestones exposed to salt, SA, and NA. According to MIP analysis, the pore size distribution curves became multimodal, and the pore sizes varied in the studied limestones exposed to salt, SA, and NA. The findings of our study serve as an important guide for the use of limestone as a natural stone in regions with severe weather conditions.

Keywords Limestone · Capillary water absorption · MIP · Weight · Antalya

Introduction

Natural stones used in building construction are expected to meet certain physical and mechanical requirements. Their physical properties, such as colour and texture, and mechanical properties, i.e., compressive strength, bending strength, and rupture modulus, are taken into account in the selection of natural stone as building and cover materials. The susceptibility of the materials to different atmospheric factors, such as air pollutants and salts, and their capillary water absorption capacity are other parameters considered in the use of natural stones.

Limestone has been widely used as a construction material in buildings and monument structures for hundreds of years due to its workability. Limestones vary depending on their geological structure, mineralogical and chemical composition, grain size, and textural properties. These properties lead to differences in weathering characteristics and behaviour under different environmental conditions and applications (Souza et al. 2021). Limestones are particularly vulnerable to moist weather conditions and air pollutants (SO_x and NO_x). Therefore, complex weathering processes involving physical, chemical, and biological effects are observed in limestones over time (Pápay et al. 2021; Steiger and Charola 2011; Korkanç and Savran 2015).

Water in combination with other environmental factors intensifies the degree of weathering in natural stone. When the pores of stone are filled with water, soluble salts, or air pollutants (SO_x/NO_x), natural stones weather and their mechanical are also adversely affected (Rothert et al. 2007; Cueto et al. 2009; Tomašić et al. 2011). Therefore, the pore

✉ Sevgi Çetintaş
scetintas@akdeniz.edu.tr

¹ Vocational School of Technical Sciences, Akdeniz University, Antalya, Turkey

² Department of Geology, Engineering Faculty, Afyon Kocatepe University, Afyonkarahisar, Turkey

size distribution and capillary water absorption parameters of natural stones are very important in understanding and predicting weathering.

The most common type of weathering in limestones is crystallization and dissolution of salts in the pore systems (Doehne 2002; Ruffolo et al. 2015; Al Omari et al. 2016). Soluble salts delay drying by increasing the critical water content in capillary cracks and/or pores. Once the water evaporates, the salts crystallize and form unsightly stains, blooms, flakes, or bands on the stone surface (Siegesmund and Dürrast 2011; Charola 2000; Benavente et al. 2007). This process results in the surface degradation of limestone over many crystallization/dissolution cycles of various soluble salts in dry and wet weather (Grossi and Brimblecombe 2007; Monna et al. 2008; Pířkryl et al. 2017). Pore size distribution is a key parameter affecting the damage caused by salts to stone, with particularly detrimental effects on stone strength (Nicholson 2001; Yu and Oguchi 2010; López-Doncel et al. 2016).

Weathering is a complex process that accelerates the degradation of rocks in the presence of soluble salts and air pollutants, such as sulfur dioxide (SO_2), nitrogen oxide (NO_x), carbon monoxide (CO), carbon dioxide CO_2 , and atmospheric particulate matter (PM) (Molina et al. 2017; De la Fuente et al. 2011; Steiger and Charola 2011; Ozga et al. 2011; Spezzano 2021). Sulphuric acid (H_2SO_4) acts on the limestone in the presence of moisture and causes the formation of calcium sulfide hemihydrate ($\text{CaSO}_3 \cdot 0.5 \text{H}_2\text{O}$) and gypsum ($\text{CaSO}_4 \cdot 2\text{H}_2\text{O}$) on the surface of stones (Rodríguez-Navarro and Sebastian 1996). Gypsum and calcium sulfide affect the presence and distribution of hemihydrate and cause deformations on the surface of natural stone (Böke et al. 2002; Malaga-Starzec et al. 2003). Weathering occurs by the action of gaseous pollutants on stone surfaces, it varies in dry and wet climates, and it depends on temperature and humidity conditions (Grossi and Murray 1999; Elfving et al. 1994; Böke et al. 1999; Luque et al. 2013; Lan et al. 2005; Olaru et al. 2010). Major air pollutants, such as NO and NO_2 , produce strong acids such as HNO_2 and HNO_3 in the presence of water, and these acids cause deterioration of the surface of natural stone. Studies assessing the effects and weathering mechanisms of nitrogen oxide on natural stone are quite limited (Kirkitsos and Sikiotis 1995, 1996). Nitrogen oxides act mainly as catalysts for SO_2 oxidation during dry and wet deposition processes (Massey 1999; Haneef et al. 1992, 1993; Bai et al. 2006). The secondary crystallization of calcium sulfate and calcium nitrate has been reported to be much higher in wet conditions (Allen et al. 2000). Ageing tests carried out in mixed acid atmospheres under laboratory conditions showed that the effects caused by HNO_3 and H_2SO_3 acid mixtures on stone surfaces occurred faster than with pure NO_2 under wet atmospheric conditions (Vazquez et al. 2016). Recent studies have focused on

the capillary water absorption–pore relationship in natural stone and the effects of weathering due to salt and air pollutants on mineralogical, physical, and mechanical properties. The findings of these studies show that salt-induced weathering in limestones is generally a function of various mineralogical–petrographical and physico-mechanical parameters, such as mineral type and distribution, strength, freeze–thaw resistance, ultrasonic velocity, roughness, and colour (Espinosa Marzal and Scherer 2008; Barbera et al. 2012; Derluyn et al. 2014). Many studies have discussed the importance of capillary water absorption and pore distribution and their effects on weathering. According to these studies, pore size distribution has an effect on permeability and is also influenced by rock texture (Lucia 1983). Small pore sizes in rocks produce low water absorption coefficient values (Benavente et al. 2002), and this coefficient may be inversely proportional to rock strength. The pore structure effect strongly affects the water absorption coefficient when used as a strength indicator (Benavente et al. 2004, 2007). Various studies on weathering processes due to air pollutants have noted that open porosity and surface weathering lead to a loss of material in different rock types, resulting in changes in colour and surface roughness (Tecer 1999; Vazquez et al. 2016; Çetintaş and Akboğa 2020).

Although the effects of the capillary water absorption coefficient, pore size distribution, salt crystallization, and air pollutants (SO_x and NO_x) on the weathering of limestones have been addressed individually in many studies, a few studies have assessed the collective action of such effects on weathering processes.

The aim of our study is to elucidate the decomposition mechanisms and physical changes that occur due to salt and air pollutants by observing the changes in capillary water absorption and porosity in limestones from the Antalya region. The variations in the capillary water absorption coefficient and pore size distribution of the studied limestones were determined based on weathering tests (salt crystallization and air pollutants), and then, the results were interpreted and discussed according to physical properties (weight and microstructure).

Materials and methods

For the laboratory experiments, three limestones were obtained from marble plants in the Antalya region. Limestone characterization is necessary to understand the behaviour of the stone in the presence of different factors that play an important role in the weathering process. For this reason, simulated weathering tests were conducted on the Antalya limestones to determine the changes in the properties of the limestones due to weathering. In the petrographical characterization of the limestones, thin sections were first

prepared for polarizing light microscopy (PLM) investigations. The petrographical and micromorphological features of the studied samples were examined using a Nikon Eclipse 2V100POL polarizing microscope, and the resulting mineralogical and petrographic descriptions are given in Table 1. A geochemical analysis of the limestones was conducted using XRF (X-ray fluorescence spectrometry), and the results of the geochemical analysis are presented in Table 2.

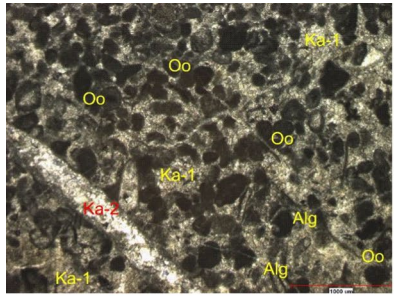
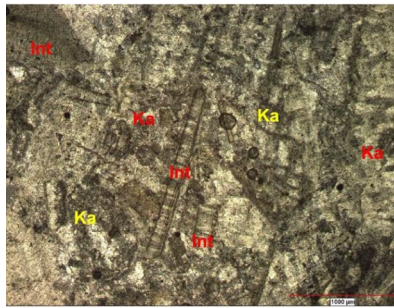
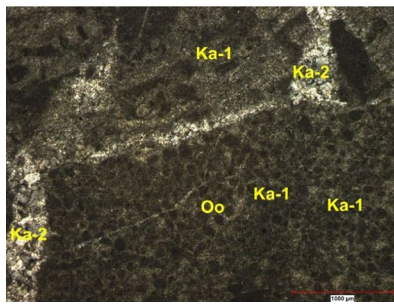
The resistance to salt crystallization (TS EN 12370) and ageing through the action of H₂SO₃ and HNO₃ (TS EN 13919) were determined based on the methods described in standards to identify changes in limestones under different atmospheric conditions (TS EN 13919 2004; TS EN 12370 2020). For the determination of resistance to salt crystallization, seven samples 40×40×40 mm in size were prepared, and one of these was used as the reference sample. The samples were left in a 14% sodium sulphate decahydrate solution (14 g Na₂SO₄·10H₂O per 86 g of deionized water) for 2 h at

Table 2 Geochemical analysis of the limestone samples

Chemical composition (wt%)	Hera Beige	Myra Beige	Crema Bella
CaO	54.57	54.78	54.89
SiO ₂	0.08	0.14	0.09
Al ₂ O ₃	0.03	0.06	0.03
MgO	0.58	0.52	0.32
P ₂ O ₅	0.02	0.01	0.00
Na ₂ O	0.01	0.03	0.02
Fe ₂ O ₃	0.04	0.03	0.03
LOI (CO ₂ , H ₂ O)	44.62	44.35	44.58
Total	99.95	99.92	99.96

20 ± 0.5 °C, and then, the limestones were removed from the solution and dried in an oven for at least 16 h. The samples were cooled at room temperature for 2.0 ± 0.5 h before being

Table 1 The mineralogical and petrographical descriptions of the limestones from the Antalya region

Sample Name	The PLM Photos of the samples	Description
Hera Beige (HB)		Micritic calcite grains have an oolitic texture. There are capillary cracks in the rock. Very thin cracks are filled with calcite. The limestone is an intramicrite. (Ka-1: Calcite, Oo: Oolite, Ka-2: Sparicalcite, Alg: Algae)
Myra Beige (MB)		Intraclasts are predominant in the rock. Very few porous sparite calcite veins are observed in some sections. Grain size ranges from 2.0–7.9 µm (micron). The limestone is an intramicrite. (Ka: Calcite, Oo: Oolite, Ka-2: Sparicalcite, Int: İtraklas)
Crema Bella (CB)		Micrite calcite crystals and an oolitic texture can be observed, as well as sparicalcite grains. The micritic grains in the rock are in the 2.0–2.8 µm range, while the sparicalcite grains measure 3.5–22.3 µm. (Ka-1: Calcite, Oo: Oolite, Ka-2: Sparicalcite, Int: İtraklas, Por: Pore)

reimmersed in a cold sodium sulphate solution. The process was repeated 15 times, and the samples were washed with deionized water (Fig. 1a). After 15 test cycles, the samples were dried at 70 ± 5 °C. The final dry weight of the samples was measured, and the relative mass difference (decrease or increase in mass) was calculated.

For the determination of resistance to ageing through the action of H_2SO_3 and HNO_3 , experiments were carried out in accordance with the procedure specified in TS EN 13919. For each experiment, seven samples $120 \times 60 \times 10$ mm in size were selected from different limestones, and the mass of the dry samples was measured (m_0). Prior to the ageing tests, the samples were immersed in water (20 ± 5 °C) at atmospheric pressure for 24 h. SA solution (150 ± 10 mL deionized water and 500 ± 10 mL H_2SO_3 acid) was prepared for the determination of resistance to ageing through the action of H_2SO_3 (sulphurous acid, solution in water containing 5–6% by mass of sulfur dioxide), and NA solution (150 ± 10 mL deionized water and 500 ± 10 mL HNO_3 acid) was prepared for the determination of resistance to ageing through the action of HNO_3 (nitric acid, solution in water containing 5–6% by mass of nitrogen dioxide). Each stone was placed in a test container without direct contact with the solution (Fig. 1b). The samples were kept at different concentrations of the SA and NA solutions in the test container and were removed from the container after 21 days, washed with deionized water, and dried (70 ± 5 °C) again. The final mass (m_1) of the dry sample was measured, and the change in mass was calculated with a precision of 0.01%.

Before and after the various atmospheric tests (weathering tests), the capillary water absorption coefficient of the limestone samples was measured in accordance with the TS EN 1925 standard, and a mercury porosimetry (MIP) analysis was conducted to determine the pore throat diameter distribution, which has bearing on the weathering mechanism in the study. Parameters such as pore throat diameter distribution, pore throat diameter, and pore volume were determined using an Autopore IV 9500 Micromeritics

mercury porosimeter before and after the weathering tests of the limestone samples. Then, a ZEISS scanning electron microscope (SEM) was used to determine the microtextural properties of the limestone samples.

Results and discussion

Changes in weight

Weight change is one of the primary physical parameters in the determination of material loss and/or crystal formation during the weathering of limestones. In the present study, the weight loss in the limestones was obtained after weathering (salt, SA, and NA) tests, and the weight change data are presented in Fig. 2.

Figure 2 shows that the weights of the limestones aged by salt action increased from 0.71 to 1.25%. The greatest weight increase was obtained in the Crema Bella, and the lowest weight increase was observed in the Myra Beige. The penetration of salt solution and precipitation of salt crystals in pores and capillary fissures during the ageing cycles induced an increase in weight in the limestones. Salt crystallization

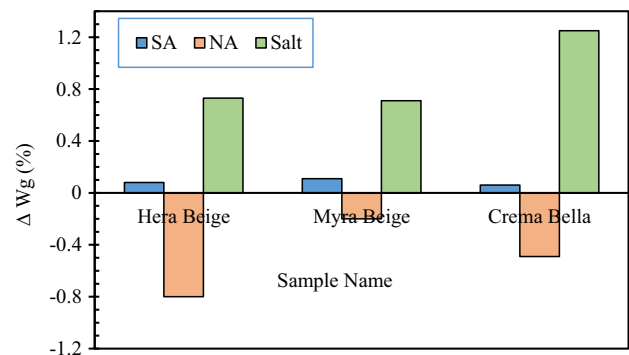


Fig. 2 Weight change in the studied samples after weathering tests

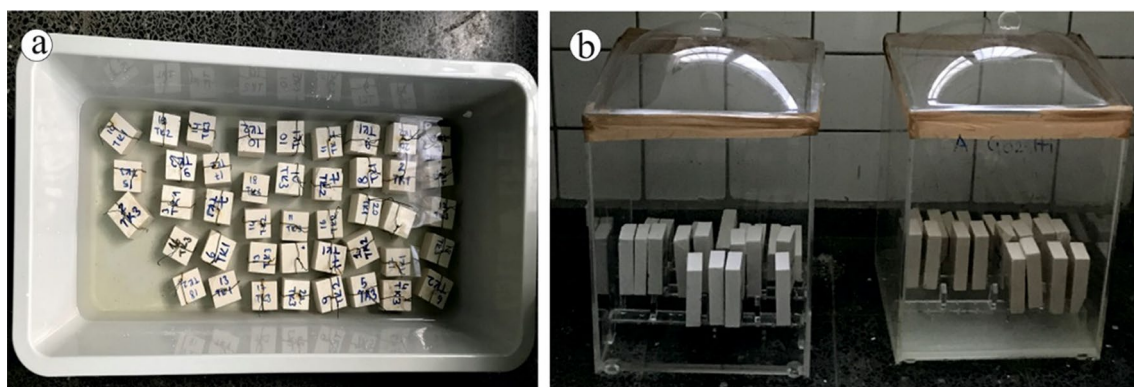


Fig. 1 Images of the tests: **a** Salt crystallization and **b** Chamber with acid solutions

due to salt ageing was generally found at the microscale and in trace amounts in SEM studies (Fig. 3).

The weight increase in Myra Beige (0.11%) was greater than that in Crema Bella (0.06%). The crystallization of calcium sulfide hemihydrate ($\text{CaSO}_3 \cdot 0.5 \text{H}_2\text{O}$) and gypsum

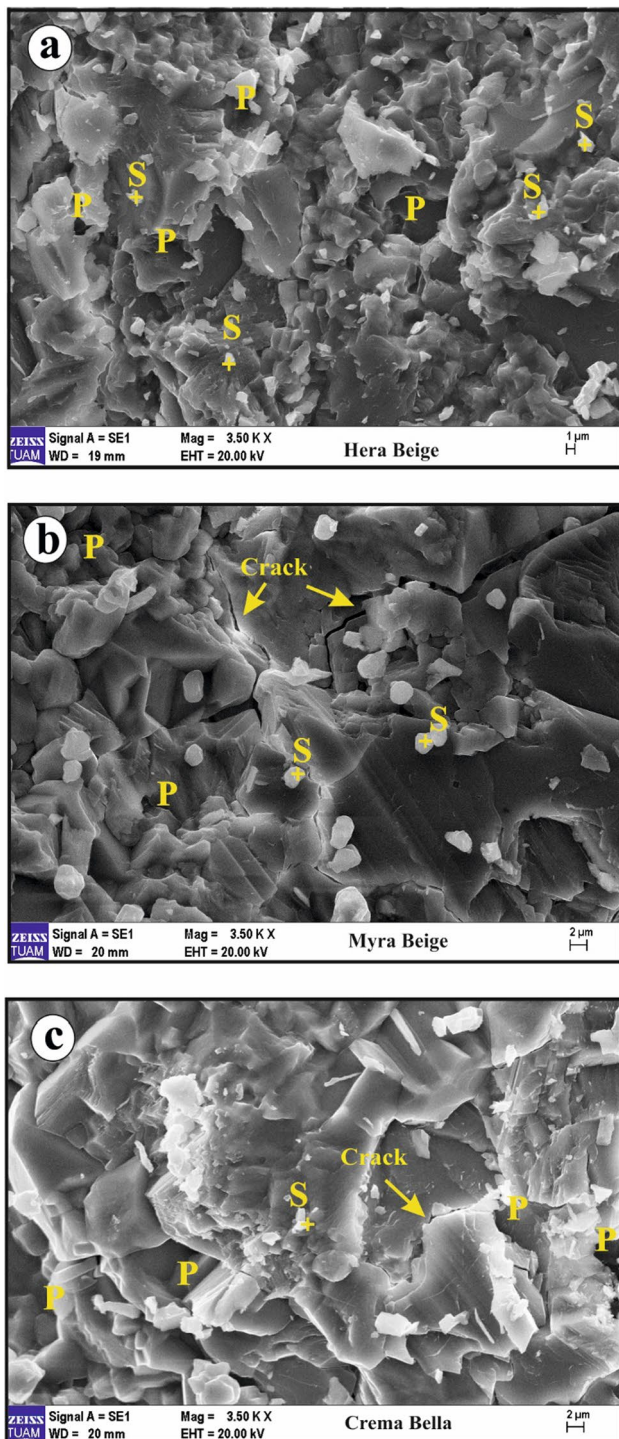


Fig. 3 SEM images of the studied limestones after salt weathering (P: pore, S: salt)

($\text{CaSO}_4 \cdot 2\text{H}_2\text{O}$) on the limestone surfaces after the SO_2 treatment resulted in weight gain without direct contact with the solution. During macroscopic examination, thin, white-coloured crust-shaped blooms were observed on the surface of the limestones (Fig. 4). The distribution and quantity of these particles varied and correlated with the mineralogical and petrographical properties of the limestones. The existence of fine-grained calcite crystals, capillary cracks, and secondary calcite fillings may lead to more rapid weathering through the action of acid. The conversion of CaO to CaSO_4 occurs rapidly in small calcite crystals (Wang et al. 2015). Secondary gypsum crystals were identified in surrounding smaller calcite crystals in SEM investigations (Fig. 5).

Ageing in an NO_2 -laden atmosphere induced a reduction in the weight of the studied limestones. The greatest weight loss was found in Hera Beige (0.80%), and the weight losses of Crema Bella and Myra Beige were 0.49% and 0.20%, respectively. The SEM studies revealed that the surface of the limestones had deteriorated as a result of the acidity of the NO_2 -containing atmosphere (Fig. 6). Secondary minerals were not detected after acid treatment. However, a porous structure was formed along the laminas and fissures. Signs of physical weathering, such as fracturing and disconnections, were observed in the capillary cracks along the secondary calcite crystals. The limestones also included veins with secondary calcite (sparite) fillings in different directions. The rock matrix had a homogeneous micrite texture with low porosity. According to the previous studies, the main causes of disintegration and weathering in limestones are the presence of secondary calcite veins and micritic textures (Barnos et al. 2020; Freire-Lista et al. 2021).

Although the NA cycle in the laboratory was more effective than natural environmental conditions, weight loss in the NA treatment limestones was less than 1.0%, which is considered minimal.

Impact on capillary absorption

The coefficient of capillary water absorption (CCWA) expresses how quickly a limestone absorbs water when it is placed in contact with water. The results of the coefficient of capillary water absorption based on weathering tests are shown in Table 3, and illustrations of capillary water absorption are presented in Fig. 7. The CCWA values increase from 0.46, 4.35, and 0.27 $\text{g/m}^2\sqrt{\text{s}}$ (in the reference samples) to 0.93, 4.74, and 0.49 $\text{g/m}^2\sqrt{\text{s}}$ (in the salt-treated samples) after the salt crystallization tests. The Hera Beige and Crema Bella samples reached maximum saturation after the first 30 min, as shown in Fig. 7a, but water absorption in the Myra Beige continued until the end of the test. The increase in the CCWA occurs, because the surface tension results in salt crystallization. Because the salt crystals in the pores weight down the pore walls, internal stress is created

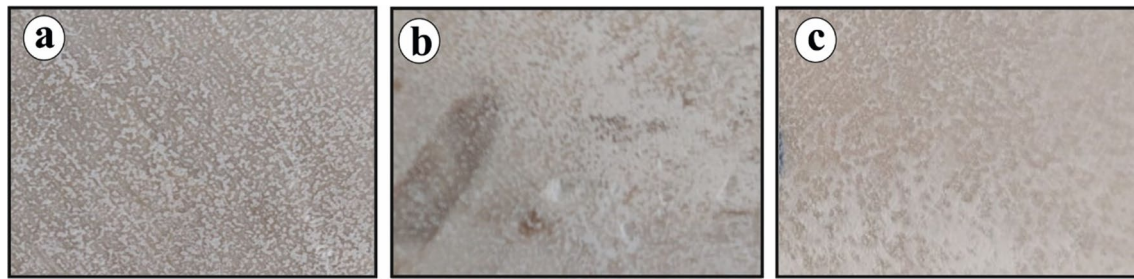


Fig. 4 Macroscopic observations of limestones after SA treatment: **a** Hera Beige, **b** Myra Beige, and **c** Crema Bella

in the stone, resulting in capillary cracks and increased porosity (Angeli et al. 2008; Dinçer and Bostancı 2019). The CCWA increases due to capillary fissures or pores after physical weathering. However, the CCWA varies depending on important factors such as environmental conditions, the amount of salt in the stone, the properties of the pore network, and salt concentration.

In the SA tests, the CCWA values of the Hera Beige and Crema Bella also increased from 1.57 to 1.72, whereas those of the Myra Beige decreased from 4.35 to 3.15 $\text{g/m}^2\sqrt{\text{s}}$ during weathering. The surface properties of limestones deteriorate under the acidic effect of SA. The type and degree of weathering and secondary mineral types change depending on the difference in the mineralogical and petrographic properties of the rocks (Scrivano et al. 2018; Israeli and Emmanuel 2018) and often lead to the formation of pores and the decomposition of minerals (Janvier-Badosa et al. 2014). The secondary mineral fillings in the pores cause a decrease in the CCWA values following mineral formation on the surface. The variation in the CCWA values of the studied limestones confirms the results of previous studies.

Figure 7c shows the variation in the capillary water absorption of the reference and NA acid-treated samples. The CCWA values of Hera Beige, Myra Beige, and Crema Bella were 1.21, 5.27, and 1.02 $\text{g/m}^2\sqrt{\text{s}}$, respectively. Capillary water absorption in Hera Beige and Crema Bella reached saturation after 30 min and remained stable until the end of the test period in the reference and acid-treated samples (Fig. 7). However, water absorption (g/m^2) increased in the reference and acid-treated samples of Myra Beige. These findings indicate prove that limestones of the same origin may show different water absorption tendencies due to different physical and mineralogical properties (pore network systems, mineral sizes).

The capillary water absorption illustrations of the weathering tests for the studied limestones are presented in Fig. 8. The values of the capillary water absorption obtained during the weathering tests of the Hera Beige sample remained stable between 60 and 294 $\sqrt{\text{s}}$ after capillary water absorption increased rapidly from 8 to 42 $\sqrt{\text{s}}$. The capillary water absorption coefficient expresses how quickly a stone can

absorb water when it comes into contact with water. In this case, water absorption was fast in Hera Beige, in the range of 8–42 $\sqrt{\text{s}}$.

According to the different weathering tests, the Hera Beige sample had the highest capillary water absorption after SA treatment, but the Crema Bella sample showed similar capillary water absorption after three weathering tests (Fig. 8a, c). The values for capillary water absorption in Myra Beige increased until the end of the test, and saturation was not reached during the weathering tests (Fig. 8c). Microporous structures can easily absorb solutions through capillary action, and the presence of salt crystals in limestone enhances the crystallization pressure in the pores at the microscale (Rijniers et al. 2005; Van et al. 2007). While the porosity dramatically decreased under the action of salt at the beginning, an increase in porosity was observed after 15 cycles. Pores that were disconnected from the outer surface could not be detected, but the internal pressure created by salts or acids can lead to the formation of new fissures connecting new pores and the open pore structure (La Russa et al. 2013). The porosity increased in the Myra Beige sample after the weathering tests, and this increase was confirmed by the MIP measurements.

Change in pore size

Porosity and pore throat distribution may have an impact on the strength of rocks. These properties were detected using the MIP technique. The MIP data of the reference and acid-treated (salt, SA, and NA tests) samples were compared to determine the change in porosity and pore throat distribution of the limestones with the weathering tests. The results of the average pore diameter, open porosity, apparent and bulk density, and pore size distribution (%) (calculated according to test results) as determined by mercury porosimetry for the studied limestones are presented in Table 4.

The MIP analysis revealed that the porosity of Hera Beige was 0.64% in the reference sample and 0.50, 0.61, and 0.66% after the salt, SA, and NA tests, respectively. The average pore diameter increased from 2.66 μm in the reference sample to 5.60 μm after the NA test in Hera Beige.

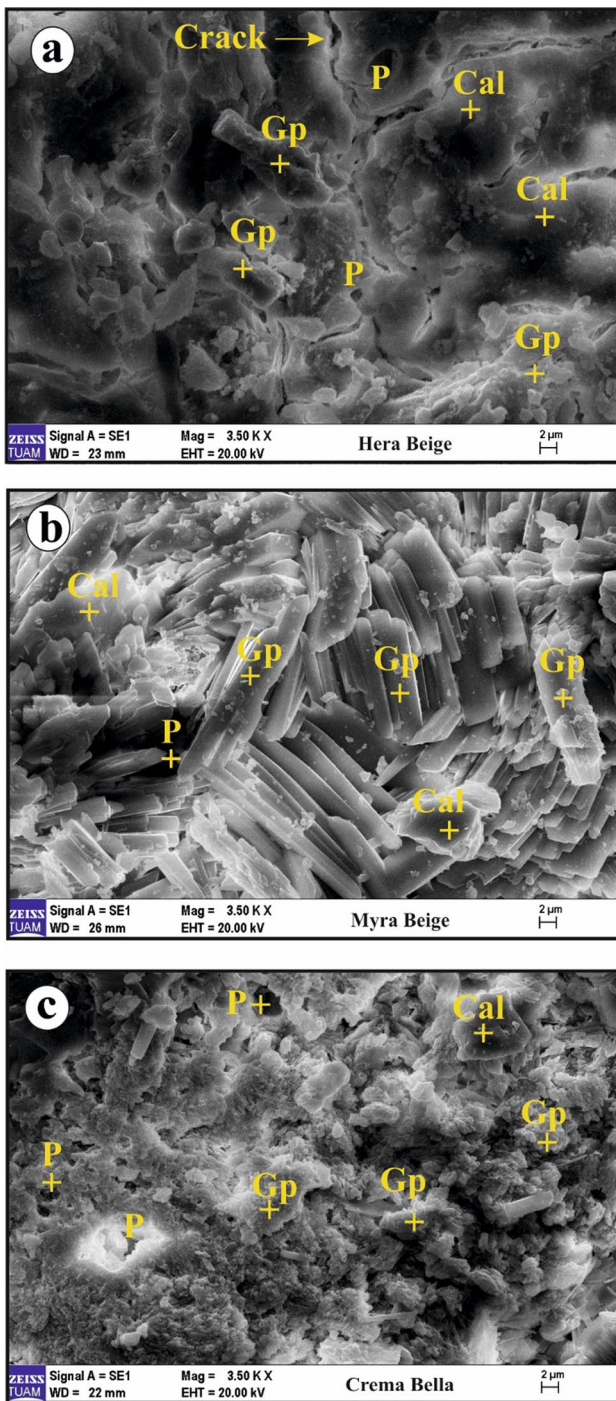


Fig. 5 SEM images after SA treatment: **a** Hera Beige, **b** Myra Beige, and **c** Crema Bella (Gp: gypsum, P: pore, and Cal: calcite)

In Myra Beige, the average pore diameter (volume) of the reference sample was 78.55 μm. However, an increase (95.95 μm) occurred after the salt test and a reduction (37.51 and 55.91 μm) was observed after the SA and NA tests, respectively, in the average pore diameter (volume). The porosity was 5.23% in the reference sample and was 6.66%,

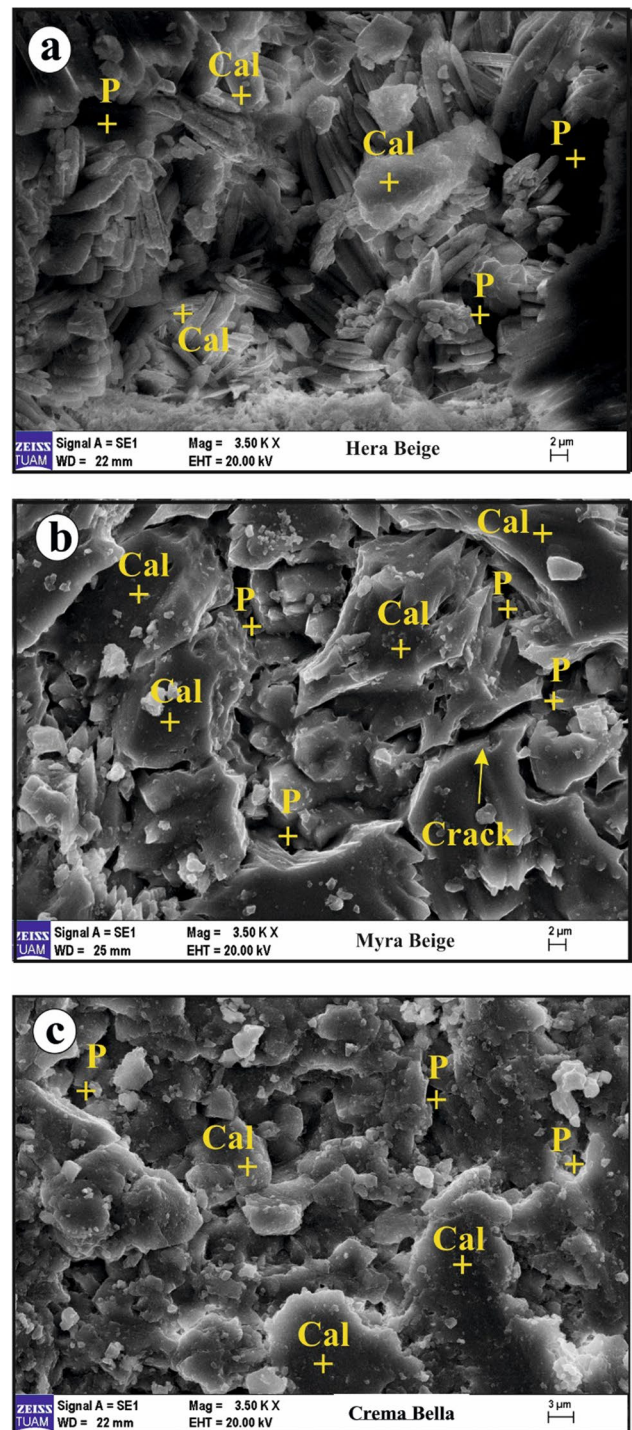


Fig. 6 SEM images of limestones after NA treatment: **a** Hera Beige, **b** Myra Beige, and **c** Crema Bella (P: pore, Cal: calcite)

5.33%, and 3.86% after the weathering tests in the MIP analysis of Myra Beige. The average pore diameter was 0.23 μm in the reference sample and increased from 0.43 to 0.47 μm after the weathering tests. While the average pore diameter (volume) was 1.17 μm in the reference sample, it decreased

Table 3 The results of the coefficient of capillary water absorption (CCWA) based on weathering tests

	Capillary water absorption coefficient ($\text{g/m}^2\sqrt{\text{s}}$)
Hera Beige ref	0.46
Hera Beige salt	0.93
Hera Beige SA	1.57
Hera Beige NA	1.21
Myra Beige ref	4.35
Myra Beige salt	4.74
Myra Beige SA	3.15
Myra Beige NA	5.27
Crema Bella ref	0.27
Crema Bella salt	0.49
Crema Bella SA	1.72
Crema Bella NA	1.02

by 0.76–1.02 μm after the weathering tests. The spherical volume decreased after weathering of Sabucina rocks due to salt crystallization in the microtextural and microstructural examinations conducted by Barone et al. (2015). The decrease in the pore diameter volume of Myra Beige after the weathering tests confirmed that the spherical volume available for mercury decreased due to new crystal formation or pore deterioration. According to the MIP results of Crema Bella, the porosity decreased from 1.31% in the reference sample to 0.45% and 0.88% after the weathering tests. The average pore diameter increased from 0.02 μm (in the reference) to 19.48, 1.08, and 11.24 μm after the salt, SA, and NA tests, respectively. A similar change was observed in the average pore diameter (volume) of Crema Bella.

In a study by Angeli et al. (2008), a comparison of unweathered and weathered pore size distribution curves provided information on the weathering mechanism induced by salt. Based on their results, if salt crystals fill a pore entrance, the modal pore radius remains low, and spherical porosity remains unchanged in the weathered samples. The degree of filling of salt crystals in pores has an effect on the pore size mode and spherical volume. Partial salt filling ensured a fixed pore mode and a lower spherical volume. However, complete filling of the pore entrance and partial filling of the pore interior by salt crystals induced a decrease in the modal pore size and spherical volume.

The pore size distribution curves of the studied limestones are presented in Fig. 9. After the tests, the studied limestones had a multimodal pore size distribution. Differences in pore sizes were observed between the reference and weathered samples. The pore size modes between 0.2 and 0.5 μm and 50 and 346 μm reached 2–3 μm after salt crystallization. This new pore mode shows that salt crystals formed new pores in Hera Beige (Fig. 9a). The post-test pore size mode

was in the range of 0.03–8 μm , and a reduction in spherical volume was observed in Myra Beige (Fig. 9b). An increase in spherical volume was observed in the 20–30 μm pore size mode. However, the pore size did not change, and the spherical volume decreased in the 50–346 μm pore size range. The pore size mode was not changed, but the spherical volume decreased in the range of 9–345 μm after the weathering test in Crema Bella. The pore ranges of 0.004–0.005, 0.01–0.02, 0.03–0.05, 0.07–0.14, and 0.6–1 μm in Crema Bella could not be identified after the weathering test (Fig. 9c). The variation in pore range was interpreted as the disappearance or filling of microsized pores with salt crystals during the weathering process.

The graphics of the pore size distribution curves show that the pore sizes changed to multimodal based on the SA test (Fig. 10). New pores ranging from 0.9 to 1.5 μm were found after the SA test in Hera Beige (Fig. 10a). The new pores similarly formed in the 0.14–0.20 μm and 1–2 μm ranges in Crema Bella (Fig. 10c). The modal pore size was shifted towards lower values along with a decrease in incremental pore volume in the range of 0.15–0.20 μm in Hera Beige. The pore size mode between 6 and 346 μm was not changed, but the incremental pore volume shifted towards lower values. The incremental pore volume decreased in the pore size range of 9–346 μm , and the pore size did not change in Crema Bella. The multiple modes confirmed the existence of gypsum minerals that formed as a result of the interaction of calcite minerals with SA. Secondary gypsum crystals filled the pores, causing a decrease in incremental pore volume. The destructive and abrasive effect of SA gave rise to the formation of new pores (Fig. 5). The pore size mode of the weathered test sample was in the range of 0.03–8 μm , the incremental pore volume decreased, and the pore size range increased in Myra Beige (Fig. 10b). Pore size was not changed, but the incremental pore volume decreased in the pore size range of 9–346 μm . The increase in pore size resulted in the formation of more pores through the action of SA. Incremental pore volume was reduced due to the presence of the newly formed crystals.

The pore size distribution curves in the NA weathering test show marked changes and differences in pore sizes (Fig. 11). New pores or fissures in the range of 0.6–7 μm were observed after the NA test, the pore size mode in the range of 30–345 μm was not changed, and the incremental pore volume also decreased in Hera Beige (Fig. 11a). From the absence of pore volumes in the range of 0.2–0.5 μm after the NA test, it can be concluded that the pore sizes of the rocks decreased, and newly formed porous structures were also observed in SEM studies (Fig. 6). Under the action of concentrated solutions, small pores and microcracks begin to grow during the cycle and decompose the limestones. The incremental pore volume increased both in the range of 0.05–8 μm and in the range of 9–346 μm , and the

Fig. 7 Illustrations of capillary water absorption: **a** salt crystallization, **b** SA solution, and **c** NA solution. Abbreviations: *Ref HB* reference Hera Beige, *Ref MB* reference Myra Beige, *Ref CB* reference Crema Bella, *Salt HB* after salt crystallization test of Hera Beige, *Salt MB* after salt crystallization test of Myra Beige, *Salt CB* after salt crystallization test of Crema Bella, *SA HB* after SA solution test of Hera Beige, *SA MB* after SA solution test of Myra Beige, *SA CB* after SA solution test of Crema Bella, *NA HB-NA MB* after NA solution test of Myra Beige, *NA CB* after NA solution test of Crema Bella

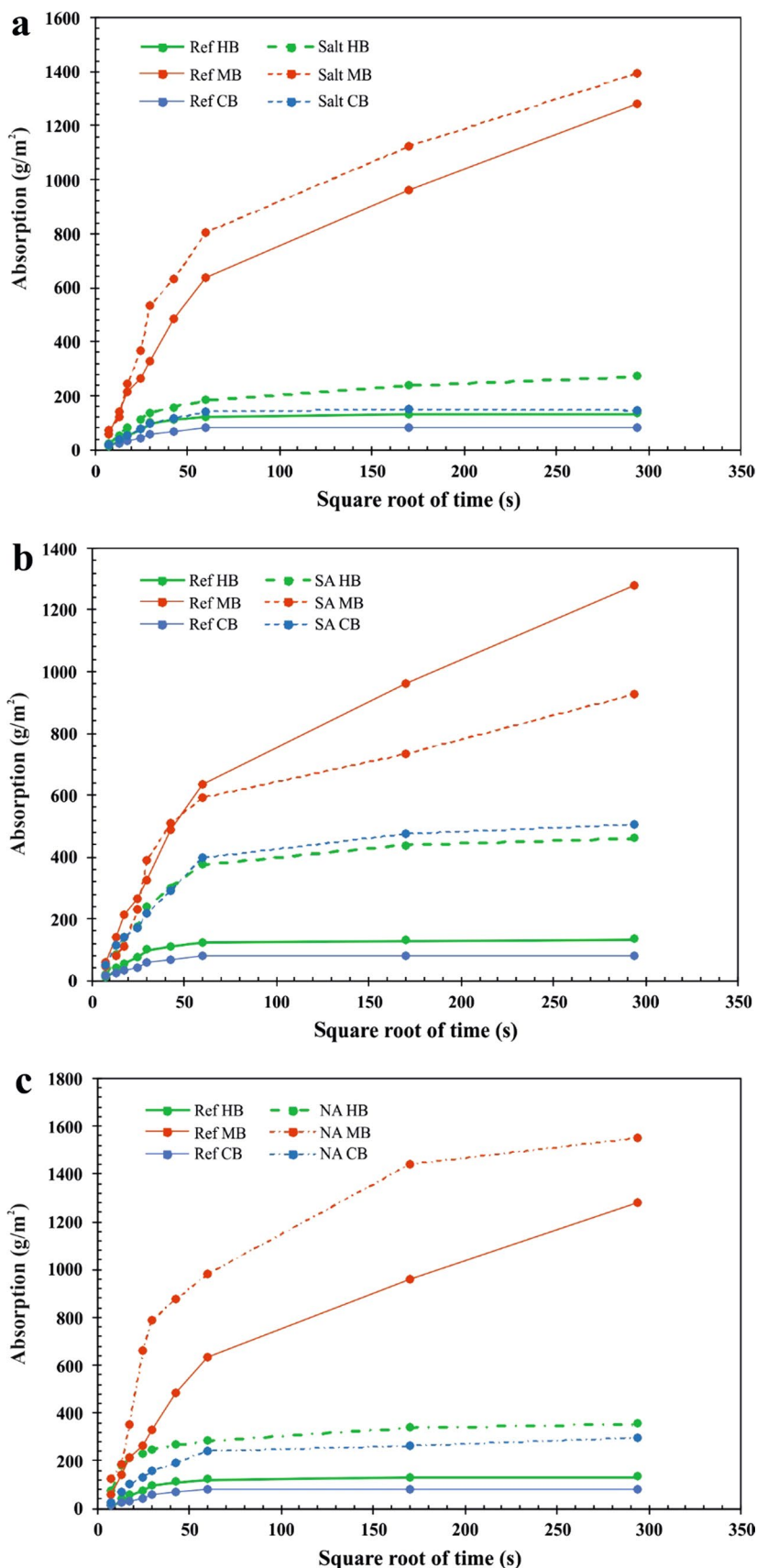


Fig. 8 Capillary water absorption illustrations of the weathering tests for the studied limestones: **a** Hera Beige, **b** Myra Beige, and **c** Crema Bella. Abbreviations: *Salt HB* after salt crystallization test of Hera Beige, *SA HB* after SA solution test of Hera Beige, *NA HB* after NA solution test of Hera Beige, *Salt MB* after salt crystallization test of Myra Beige, *SA MB* after SA solution test of Myra Beige, *NA MB* after NA solution test of Myra Beige, *Salt CB* after salt crystallization test of Crema Bella, *SA CB* after SA solution test of Crema Bella and *NA CB* after NA solution test of Crema Bella

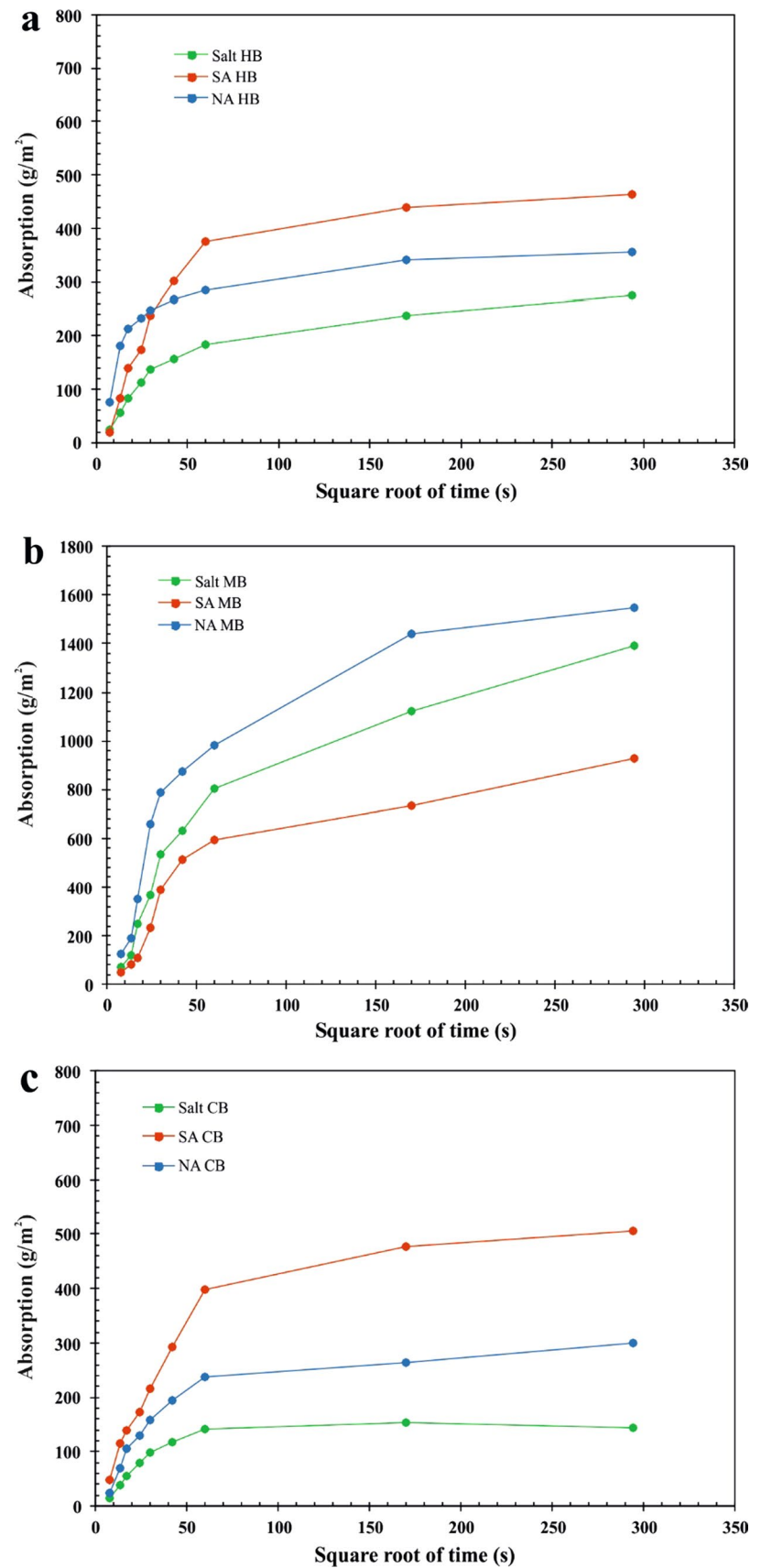


Table 4 The pore size distribution values of the studied limestones

	Total intrusion volume (mL/g)	Total pore area (m ² /g)	Median pore diameter (volume) μm	Median pore diameter (area) μm	Average pore diameter μm	Bulk density at 0.52 psia (g/mL)	Apparent (skel-etal) density (g/mL)	Porosity %
Hera Beige Ref	0.0024	0.0040	78.5530	0.4210	2.6640	2.6482	2.6653	0.6435
Hera Beige Salt	0.0019	0.0020	95.9540	0.3930	4.2660	2.6597	2.6730	0.5000
Hera Beige SA	0.0023	0.0030	37.5090	1.1780	2.9050	2.6451	2.6612	0.6068
Hera Beige NA	0.0025	0.0020	55.9130	0.9190	5.6000	2.6479	2.6655	0.6598
Myra Beige Ref	0.0206	0.3600	1.1720	0.0270	0.2290	2.5396	2.6797	5.2270
Myra Beige Salt	0.0269	0.2350	0.7580	0.2250	0.4580	2.4744	2.6509	6.6576
Myra Beige SA	0.0213	0.1820	0.8490	0.2090	0.4670	2.5060	2.6471	5.3302
Myra Beige NA	0.0152	0.1400	1.0230	0.1640	0.4340	2.5358	2.6378	3.8646
Crema Bella Ref	0.0050	1.1130	48.0660	0.0140	0.0180	2.6369	2.6719	1.3092
Crema Bella Salt	0.0017	0.0000	112.5270	0.6810	19.4840	2.6841	2.6963	0.4542
Crema Bella SA	0.0033	0.0120	2.1370	0.4210	1.0820	2.6595	2.6830	0.8800
Crema Bella NA	0.0020	0.0010	93.4700	1.8480	11.2390	2.6528	2.6668	0.5200

incremental pore volume decreased in the range of 4–8 μm in Myra Beige (Fig. 11b). New pores or fissure were formed in the range of 2–4 μm , the pore size was not changed in the range of 8–346 μm , and the incremental pore volume decreased in Crema Bella (Fig. 11c).

The gypsum was a sequential reaction product and formed as a result of the dissolution of calcite by acids. This conversion is known as the acidity effect and occurs by the substitution of carbonate with sulfates (Gibeaux et al. 2018). The MIP analysis revealed new pore formation in limestones that were exposed to air pollutants (SA and NA), the pore size was not changed, and the spherical volume decreased due to the dissolution of calcite. The porous network of rocks affects dissolution and crystallization patterns. The good pore connection leads to an increase in porosity due to rock dissolution by acid rain. Dissolution occurs mainly on the surface in the case of low connectivity, even if the pore distribution changes (Eyssautier-Chuine et al. 2016). This phenomenon accounts for the difference in the grain size distribution values of the reference samples used in the study and the values after the weathering tests, namely, the increase and decrease in porosity (%).

Conclusion

Limestone, as a building material, is subject to weathering by salt and air pollutants (SA and NA). In the present study, laboratory tests were carried out to evaluate the weathering behaviours of three limestones from the Antalya region

under the effects of salt and air pollutants SA and NA through an evaluation of their capillary water absorption and pore distribution characteristics. Capillary water absorption, weight change, and mercury porosimetry analyses were carried out to determine physical and microstructural changes in the limestones during the tests using scanning electron microscope (SEM) examinations. The experimental results obtained from the study are presented below.

Weight increased in the salt and SA weathering tests. No change was observed at a macroscopic scale due to the effects of salt. However, salt crystals developed in the pores at the microscopic scale. The reaction of the SO_2 atmosphere in the test chamber with the limestone influenced the presence and distribution of calcium sulfite hemihydrate and gypsum on the surface of the limestones and resulted in weight gain without direct contact with the solution. At a macroscopic scale, thin, white crust-shaped blooms formed on the surface of the studied limestones. The reduced weights of the limestones under the action of NA and the formation of the porous structure observed under microscale examination confirmed the loss of material. An evaluation of the strength of the limestones as a building material in our study revealed the Antalya limestones to be “very strong” according to a classification system based on resistance to salt attack. Classifications according to the effect of air pollutants do not exist. However, the studied limestones are considered to be very strong due to their low weight loss (< 1%) after exposure to H_2SO_3 and HNO_3 solutions.

The values for capillary water absorption increased in the limestones after the salt weathering tests, since the salt

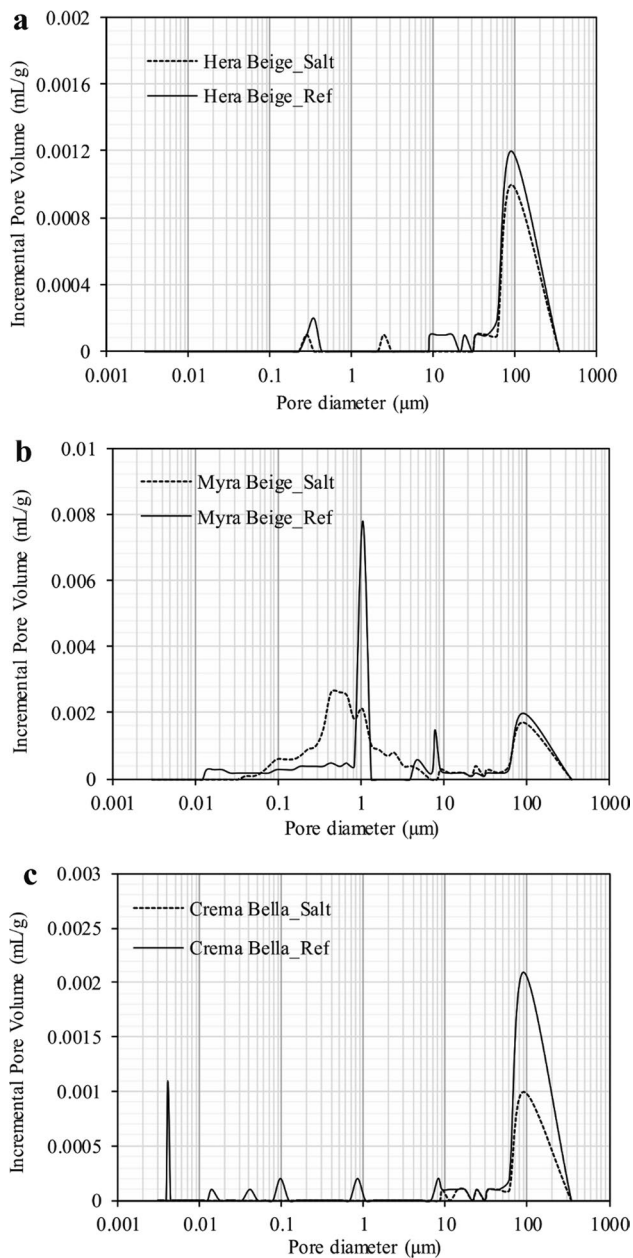


Fig. 9 The pore size distribution curves of studied limestones with salt tests: **a** Hera Beige, **b** Myra Beige, and **c** Crema Bella

increased surface tension. The formation of new pores in the structure of the studied limestones under the action of SA and NA increased the capillary water absorption coefficient. Secondary mineral filling of the pores in the limestones resulted in decreased water absorption and the formation of secondary minerals on the rock surface.

After the limestone weathering tests, the pore size distribution curves became multimodal, and the pore sizes varied. Gypsum minerals were formed as a result of the interaction of calcite minerals with SA and filled the pores, resulting in decreased incremental pore volumes. The destructive and

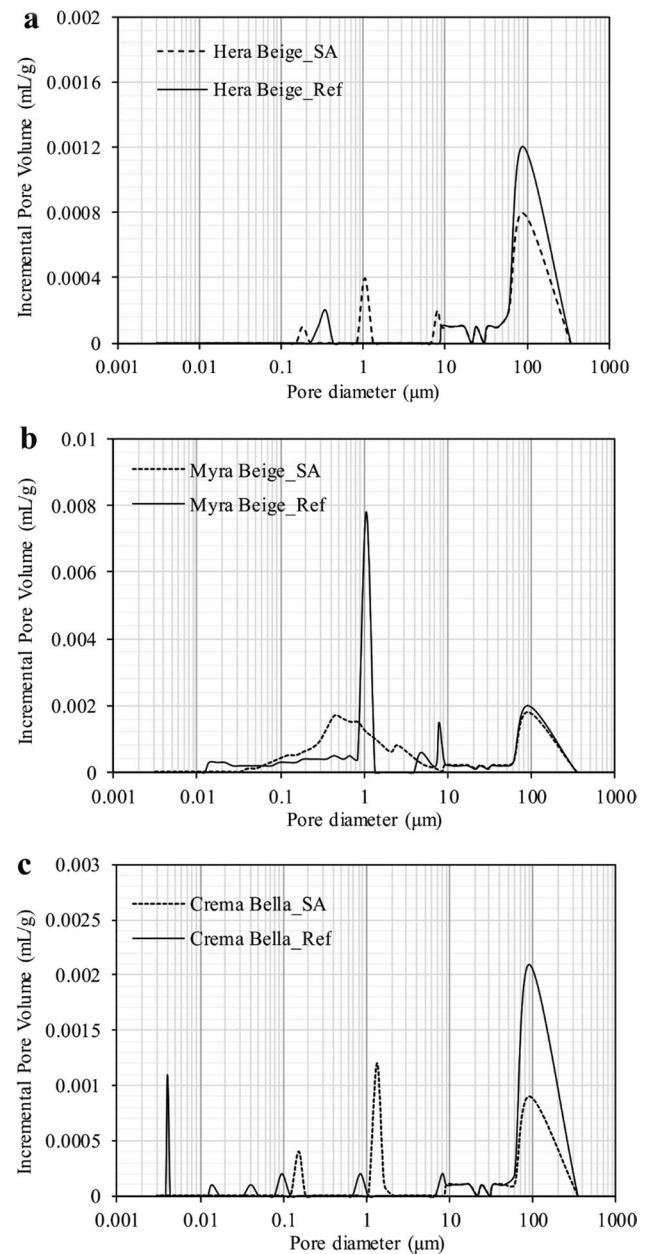


Fig. 10 Pore size distribution curves with SA tests: **a** Hera Beige, **b** Myra Beige, and **c** Crema Bella

abrasive effect of the weathering tests led to the formation of new pores.

According to MIP analysis of the new pores observed in the studied limestones exposed to air pollutants (SA and NA), pore size did not change due to the dissolution of calcite under the action of acid, whereas the spherical volume decreased due to the substitution of carbonate with sulfates.

To conclude, a better understanding of weathering mechanisms can be gained by determining the physical and microstructural (capillary water absorption coefficient and pore

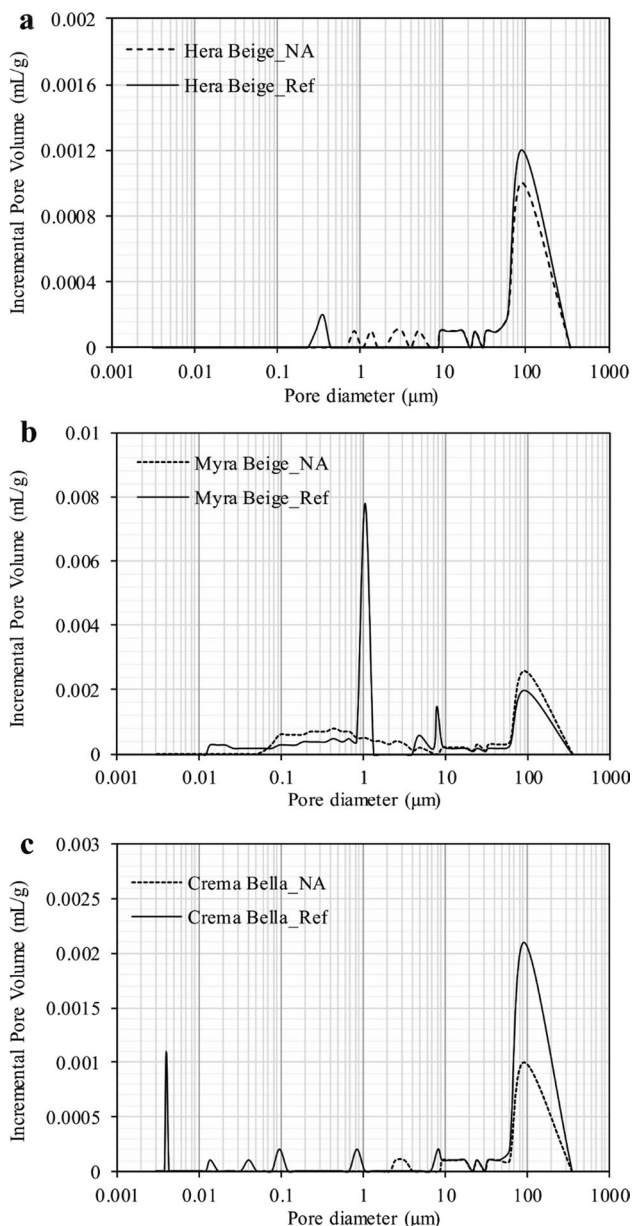


Fig. 11 Pore size distribution curves during the NA weathering tests: **a** Hera Beige, **b** Myra Beige, and **c** Crema Bella

distribution) properties of limestones during weathering tests. The approach used in our study provides significant benefits, particularly during the use of limestone as a building material in regions with harsh weather conditions.

Acknowledgements The authors would like to thank Akdeniz University Scientific Research Projects Coordinatorship for their financial support to Project No: 3443 and Adalya Marble, Batı Aegean, and Portsan marble companies for providing the samples.

Author contributions The authors would like to introduce the individual author contributions as below: SÇ: conceptualization, methodology, investigation, project administration, writing—original draft, and

writing—review & editing. MB: investigation, formal analysis, methodology, and resources. AY: investigation, methodology, and resources.

Funding Funding Coordinator of Scientific Research Projects of Akdeniz University.

Data availability Not applicable.

Declarations

Conflict of interest We all agree with the content of this manuscript and there is no conflict of interest to report. We certify that the submission is original work and is not under review at any other publication.

References

- Al Omari MMH, Rashid IS, Qinna NA, Jaber AM, Badwan AA (2016) Calcium carbonate. In: Brittain HG (ed) Profiles of drug substances, excipients and related methodology, vol 41. Academic, Burlington, pp 31–132
- Allen GC, El-Turki N, Hallam KR, McLaughlin D, Stacey M (2000) Role of NO₂ and SO₂ in degradation of limestone. *Br Corros J* 35:35–38. <https://doi.org/10.1179/000705900101501047>
- Angeli M, Benavente D, Bigas JP, Menéndez B, Hébert R, David C (2008) Modification of the porous network by salt crystallization in experimentally weathered sedimentary stones. *Mater Struct* 41:1091–1108. <https://doi.org/10.1617/s11527-007-9308-z>
- Bai Y, Thompson GE, Martinez-Ramirez S (2006) Effects of NO₂ on oxidation mechanisms of atmospheric pollutant SO₂ over Baumberger sandstone. *Build Environ* 41:486–491. <https://doi.org/10.1016/j.buildenv.2005.02.007>
- Barbera G, Barone G, Mazzoleni P, Scandurra A (2012) Laboratory measurement of ultrasound velocity during accelerated ageing tests: implication for the determination of limestone durability. *Constr Build Mater* 36:977–983. <https://doi.org/10.1016/j.conbuilmat.2012.06.029>
- Barnoos V, Oudbashi O, Shekofteh A (2020) The deterioration process of limestone in the Anahita Temple of Kangavar (West Iran). *Herit Sci* 8:1–19. <https://doi.org/10.1186/s40494-020-00411-1>
- Barone G, Mazzoleni P, Pappalardo G, Raneri S (2015) Microtextural and microstructural influence on the changes of physical and mechanical properties related to salts crystallization weathering in natural building stones. The example of Sabucina stone (Sicily). *Constr Build Mater* 95:355–365. <https://doi.org/10.1016/j.conbuilmat.2015.07.131>
- Benavente D, Lock P, García del Cura MA, Ordóñez S (2002) Predicting the capillary imbibition of porous rocks from microstructure. *Transp Porous Media* 49:59–76
- Benavente D, Garcia del Cura MA, Garcia-Guinea J, Sanchez-Moral S, Ordóñez S (2004) Role of pore structure in salt crystallization in unsaturated porous stone. *J Cryst Growth* 260:532–544. <https://doi.org/10.1016/j.jcrysgro.2003.09.004>
- Benavente D, Martinez-Martinez J, Cueto N, Garcia del Cura MA (2007) Salt weathering in dual-porosity building dolostones. *Eng Geol* 94:215–226. <https://doi.org/10.1016/j.enggeo.2007.08.003>
- Böke H, Göktürk H, Caner Saltık EN, Demirci Ş (1999) Effect of airborne particles on SO₂—calcite reaction. *Appl Surf Sci* 140:70–82
- Böke H, Göktürk EH, Caner Saltık EN (2002) Effect of some surfactants on SO₂—marble reaction. *Mater Lett* 57:935–939
- Çetintaş S, Akboğa Z (2020) Investigation of resistance to ageing by SO₂ on some building stone. *Constr Build Mater* 262(4):120341. <https://doi.org/10.1016/j.conbuilmat.2020.120341>

- Charola AE (2000) Salts in the deterioration of porous materials: an overview. *J Am Inst Conserv* 39:327–343. <https://doi.org/10.1179/019713600806113176>
- Cueto N, Benavente D, Martínez-Martínez J, García-del-Cura MA (2009) Rock fabric, pore geometry and mineralogy effects on water transport in fractured dolostones. *Eng Geol* 107(1–2):1–15. <https://doi.org/10.1016/j.enggeo.2009.03.009>
- De La Fuente D, Vega JM, Viejo F, Díaz I, Morcillo M (2011) City scale assessment model for air pollution effects on the cultural heritage. *Atmos Environ* 45(6):1242–1250. <https://doi.org/10.1016/j.atmosenv.2010.12.011>
- Derluyt H, Moonen P, Carmeliet J (2014) Deformation and damage due to drying-induced salt crystallization in porous limestone. *J Mech Phys Solids* 63:242–255
- Dinger Í, Bostanci M (2019) Capillary water absorption characteristics of some Cappadocian ignimbrites and the role of capillarity on their deterioration. *Environ Earth Sci* 78:7. <https://doi.org/10.1007/s12665-018-7993-2>
- Doehne E (2002) Salt weathering: a selective review. *Geol Soc Lond Spec Pub* 205:51–64
- Elfving P, Panas I, Lindqvist O (1994) Model study of the first steps in the deterioration of calcareous stone I. Initial surface sulphite formation on calcite. *Appl Surf Sci* 74:91–98
- Espinosa Marzal RM, Scherer GW (2008) Crystallization of sodium sulfate salts in limestone. *Environ Geol* 56:605–621. <https://doi.org/10.1007/s00254-008-1441-7>
- Eyssautier-Chuine S, Marin B, Thomachot-Schneider C, Fronteau G, Schneider A, Gibeaux S, Vazquez P (2016) Simulation of acid rain weathering effect on natural and artificial carbonate stones. *Environ Earth Sci* 75:748–767. <https://doi.org/10.1007/s12665-016-5555-z>
- Freire-Lista DM, Sousa L, Carter R, Al-Na'imi F (2021) Petrographic and petrophysical characterisation and structural function of the heritage stones in Fuwairit Archaeological Site (NE Qatar): implications for heritage conservation. *Episodes* 44(1):43–58. <https://doi.org/10.18814/epiugs/2020/0200s12>
- Gibeaux S, Thomachot-Schneider C, Eyssautier-Chuine S, Marin B, Vazquez P (2018) Simulation of acid weathering on natural and artificial building stones according to the current atmospheric SO₂/NO_x rate. *Environ Earth Sci* 77:327. <https://doi.org/10.1007/s12665-018-7467-6>
- Grossi CM, Brimblecombe P (2007) Effect of long-term changes in air pollution and climate on the decay and blackening of European stone buildings. *Geol Soc Lond Spec Publ* 271(1):117–130. <https://doi.org/10.1144/GSL.SP.2007.271.01.13>
- Grossi CM, Murray M (1999) Characteristics of carbonate building stones that influence the dry deposition of acidic gases. *Constr Build Mater* 13(3):101–108
- Haneef SJ, Johnson JB, Dickinson C, Thompson GE, Wood GC (1992) Effect of dry deposition of NO_x and SO₂ gaseous pollutants on the degradation of calcareous building stones. *Atmos Environ* 26(16):2963–2974. [https://doi.org/10.1016/0960-1686\(92\)90288-V](https://doi.org/10.1016/0960-1686(92)90288-V)
- Haneef SJ, Johnson JB, Thompson GE, Wood GC (1993) The degradation of coupled stones by wet deposition processes. *Corros Sci* 34:497–510. [https://doi.org/10.1016/0010-938X\(93\)90119-2](https://doi.org/10.1016/0010-938X(93)90119-2)
- Israeli Y, Emmanuel S (2018) Impact of grain size and rock composition on simulated rock weathering. *Earth Surf Dyn* 6:319–327. <https://doi.org/10.5194/esurf-6-319-2018>
- Janvier-Badosa S, Beck K, Brunetaud X, Al-Mukhtar M (2014) The occurrence of gypsum in the scaling of stones at the castle of Chambord (France). *Environ Earth Sci* 71:4751–4759. <https://doi.org/10.1007/s12665-013-2865-2>
- Kirkitsos P, Sikiotis D (1995) Deterioration of Pentelic marble, Portland limestone and Baumberger sandstone in laboratory exposures to gaseous nitric acid. *Atmos Environ* 29(1):77–88
- Kirkitsos P, Sikiotis D (1996) Deterioration of pentelic marble, Portland limestone and Baumberger sandstone in laboratory exposures to NO₂: a comparison with exposures to gaseous HNO₃. *Atmos Environ* 30(6):941–950
- Korkanç M, Savran A (2015) Impact of the surface roughness of stones used in historical buildings on biodeterioration. *Constr Build Mater* 80:279–294. <https://doi.org/10.1016/j.conbuildmat.2015.01.073>
- La Russa MF, Ruffolo SA, Belfiore CM, Aloise P, Randazzo L, Rovella N, Pezzino A, Montana G (2013) Study of the effects of salt crystallization on degradation of limestone rocks. *Period Di Mineral* 82(1):113–127. <https://doi.org/10.2451/2013PM0007>
- Lan TTN, Nishimura R, Tsujino Y, Satoh Y, Thoa NTP, Yokoi M, Maeda Y (2005) The effects of air pollution and climatic factors on atmospheric corrosion of marble under field exposure. *Corros Sci* 47(4):1023–1038. <https://doi.org/10.1016/j.corsci.2004.06.013>
- Lucia FJ (1983) Petrophysical parameters estimated from visual description of carbonate rocks: a field classification of carbonate pore space. *J Petrol Technol* 35:629–637
- Luque A, Yuso MVM, Cultrone G, Sebastián E (2013) Analysis of the surface of different marbles by X-ray photoelectron spectroscopy (XPS) to evaluate decay by SO₂ attack. *Environ Earth Sci* 68(3):833–845. <https://doi.org/10.1007/s12665-012-1786-9>
- López-Doncel R, Wedekind W, Leiser T, Molina-Maldonado S, Velasco-Sánchez A, Dohrmann R, Kral A, Wittenborn A, Aguillón-Robles A, Siegesmund S (2016) Salt bursting tests on volcanic tuff rocks from Mexico. *Environ Earth Sci* 75:212. <https://doi.org/10.1007/s12665-015-4770-3>
- Malaga-Starzec K, Panas I, Lindqvist JE, Lindqvist O (2003) Efflorescence on thin sections of calcareous Stones. *J Cult Herit* 4:313–318. <https://doi.org/10.1016/j.culher.2003.09.002>
- Massey SW (1999) The effects of ozone and NO(x) on the deterioration of calcareous stone. *Sci Total Environ* 227(2–3):109–121
- Molina E, Rueda-Quero L, Benavente D, Burgos-Cara A, Ruiz-Agudo E, Cultrone G (2017) Gypsum crust as a source of calcium for the consolidation of carbonate stones using a calcium phosphate-based consolidant. *Constr Build Mater* 143:298–311. <https://doi.org/10.1016/j.conbuildmat.2017.03.155>
- Monna F, Puertas A, Leveque F, Losno R, Fronteau G, Marin B, Petit C, Forel B, Chateau C (2008) Geochemical records of limestone facades exposed to urban atmospheric contamination as monitoring tools. *Atmos Environ* 42(5):999–1011. <https://doi.org/10.1016/j.atmosenv.2007.10.021>
- Nicholson DT (2001) Pore properties as indicators of breakdown mechanisms in experimentally weathered limestones. *Earth Surf Proc Land* 26:819–838. <https://doi.org/10.1002/esp.228>
- Olaru M, Aflori M, Simionescu B, Doroftei F, Stratulat L (2010) Effect of SO₂ dry deposition on porous dolomitic limestones. *Materials* 3:216–231. <https://doi.org/10.3390/ma3010216>
- Ozga I, Bonazza A, Bernardi E, Tittarelli F, Favoni O, Ghedini N, Morselli L, Sabbioni C (2011) Diagnosis of surface damage induced by air pollution on 20th century concrete buildings. *Atmos Environ* 45:4986–4995. <https://doi.org/10.1016/j.atmosenv.2011.05.072>
- Pápay Z, Rozgonyi-Boissinot N, Török A (2021) Freeze-thaw and salt crystallization durability of silica acid ester consolidated porous limestone from Hungary. *Minerals* 11:824. <https://doi.org/10.3390/min11080824>
- Přikryl R, Přikrylová J, Racek M, Weishauptová Z, Kreislová K (2017) Decay mechanism of indoor porous Opuka stone: a case study from the main altar located in the St. Vitus Cathedral, Prague (Czech Republic). *Environ Earth Sci* 76:290. <https://doi.org/10.1007/s12665-017-6596-7>

- Rijniers LA, Huinink HP, Pel L, Kopinga K (2005) Experimental evidence of crystallization pressure inside porous media. *Phys Rev Lett* 94:75503. <https://doi.org/10.1103/PhysRevLett.94.075503>
- Rodriguez-Navarro C, Sebastian E (1996) Role of particulate matter from vehicle exhaust on porous building stones (limestone) sulfation. *Sci Total Environ* 87:79–91
- Rothert E, Eggers T, Cassar J, Ruedrich J, Fitzner B, Siegesmund S (2007) Stone properties and weathering induced by salt crystallization of Maltese globigerina limestone. Building stone decay: from diagnosis to conservation, geological society. *Lond Spec Publ* 271:189–198
- Ruffolo SA, La Russa MF, Ricca M, Belfiore CM, Macchia A, Comite V, Pezzino A, Crisci GM (2015) New insights on the consolidation of salt weathered limestone: the case study of Modica stone. *Bull Eng Geol Environ* 76:11–20. <https://doi.org/10.1007/s10064-015-0782-1>
- Scrivano S, Gaggero L, Aguilar JG (2018) Micro-porosity and mineralogical features influences on decay: experimental data from four dimension Stones. *Constr Build Mater* 173:342–349. <https://doi.org/10.1016/j.conbuildmat.2018.04.041>
- Siegesmund S, Dürrast H (2011) Physical and mechanical properties of rocks. In: Siegesmund S, Snethlage R (eds) *Stone in architecture*, 4th edn. Springer, Berlin, pp 97–225
- Souza L, Menningen J, Doncel RL, Siegesmund S (2021) Petrophysical properties of limestones: influence on behaviour under different environmental conditions and applications. *Environ Earth Sci* 80:814. <https://doi.org/10.1007/s12665-021-10064-3>
- Spezzano P (2021) Mapping the susceptibility of UNESCO World Cultural Heritage sites in Europe to ambient (outdoor) air pollution. *Sci Total Environ* 754:142345. <https://doi.org/10.1016/j.scitotenv.2020.142345>
- Steiger M, Charola AE (2011) Weathering and deterioration. In: Siegesmund S, Snethlage R (eds) *Stone in architecture*, 4th edn. Springer, Berlin, pp 227–316
- Tecer L (1999) Laboratory experiments on the investigation of the effects of sulphuric acid on the deterioration of carbonate stones and surface corrosion. *Water Air Soil Pollut* 114:1–12
- Tomašić I, Lukić D, Peček N, Kršinić A (2011) Dynamics of capillary water absorption in natural stone. *Bull Eng Geol Environ* 70(4):673–680. <https://doi.org/10.1007/s10064-011-0355-x>
- TS EN 1925 (2000) Natural Stone Test Methods–Determination of Water Absorption Coefficient by Capillarity. Turkish Standards Institute, Ankara
- TS EN 13919 (2004) Natural stone test methods–determination of resistance to ageing by SO₂ action in the presence of humidity. Turkish Standards Institute, Ankara
- TS EN 12370 (2020) Natural stone test methods–determination of resistance to salt crystallization. Turkish Standards Institute, Ankara
- Van TT, Beck K, Al-Mukhtar M (2007) Accelerated weathering tests on two highly porous limestones. *Environ Geol* 52:283–292. <https://doi.org/10.1007/s00254-006-0532-6>
- Vazquez P, Carrizo L, Thomachot-Schneider C, Gibeaux S, Alonso FJ (2016) Influence of surface finish and composition on the deterioration of building stones exposed to acid atmospheres. *Constr Build Mater* 106:392–403. <https://doi.org/10.1016/j.conbuildmat.2015.12.125>
- Wang C, Chen L, Jia L, Tan Y (2015) Simultaneous calcination and sulfation of limestone in CFBB. *Appl Energy* 155:478–484. <https://doi.org/10.1016/j.apenergy.2015.05.070>
- Yu S, Oguchi CT (2010) Role of pore size distribution in salt uptake, damage, and predicting salt susceptibility of eight types of Japanese building stones. *Eng Geol* 115:226–236. <https://doi.org/10.1016/j.enggeo.2009.05.007>

Publisher's Note Springer Nature remains neutral with regard to jurisdictional claims in published maps and institutional affiliations.

Springer Nature or its licensor (e.g. a society or other partner) holds exclusive rights to this article under a publishing agreement with the author(s) or other rightsholder(s); author self-archiving of the accepted manuscript version of this article is solely governed by the terms of such publishing agreement and applicable law.